ELSEVIER

Effects of temporal flow acceleration on the detachment of microparticles from surfaces

A.H. Ibrahim, P.F. Dunn*

Particle Dynamics Laboratory, Department of Aerospace and Mechanical Engineering, University of Notre Dame, Notre Dame, IN 46556, USA

Abstract

The detachment of microparticles from surfaces subjected to various *temporal* accelerations of air was studied experimentally. Stainless microspheres, approximately 70 μm in diameter, deposited as a sparse monolayer on smooth glass substrates, were subjected to temporal accelerations ranging from 0.01 to 2.0 m/s². Higher accelerations up to 23 m/s² were investigated without particles on the surface to further characterize the temporally evolving flow. Microvideographic images of the particles on the surfaces were acquired. These were used to determine the detachment fraction of the particles versus the free-stream flow velocity at different temporal flow accelerations. For the relatively slower flow accelerations, approximately 0.3 m/s² or less, microparticle detachment was independent of acceleration to within the experimental uncertainty. For the relatively more rapid accelerations, from approximately 0.3 m/s² to at least 2.0 m/s², the flow velocity required to detach one half of the microparticles increased with acceleration. Near-wall velocity measurements supported that rapid temporal acceleration delayed the onset of turbulence, thereby affecting the boundary layer characteristics, causing a decline of turbulent bursting in the wall-layer, and, hence, suppressing the detachment process.

1. Introduction

Microparticles can be detached from surfaces by flowing air under both steady and transient conditions, including those involving the rapid acceleration of the air. This acceleration can be achieved either *spatially* (such as in a convergent duct) or *temporally* (such as during a wind gust). With spatial acceleration, the flow is driven by an imposed, non-zero, spatial pressure gradient. With temporal acceleration, the flow is driven by the change in velocity with respect to time at any given spatial location and the spatial pressure gradient is near-zero. Rapid temporal accelerations occur, for example, during the on/off cycling of HVAC (heating, ventilation and air-conditioning) systems. Increases in HVAC system velocities during initiation of the ventilation cycle produces accelerations that range typically from 0.1 to 3.0 m/s² over a period of approximately 10 s. Presently, it is not clear if previously deposited microparticles will detach and resuspend into the circulating air during such periods. These microparticles can carry formerly airborne materials, such as those containing tobacco-smoke products. Other situations involving rapid temporal flow acceleration of air

---

* Corresponding author.

E-mail address: patrick.f.dunn.1@nd.edu (P.F. Dunn).

over microparticle-laden surfaces include wind gusts and changes in wind direction over exposed soil and desert sand (Gillette, 1978), and in sampling systems designed to remove microparticles adhering to surfaces by using high-velocity, short-duration air jets (Smedley, Phares, & Flagan, 1999, 2001).

Most studies on microparticle detachment from surfaces have considered steady flows and, to a lesser extent, slowly accelerating flows. Extensive reviews on particle resuspension under such conditions have been presented by Ziskind, Fichman, and Gutfinger (1995), Nicholson (1988) and Sehmel (1980). Recent studies on particle behavior in HVAC systems include those of Sippola and Nazaroff (2003, 2004, 2005), Siegel and Nazaroff (2003), and Adam, Everitt, and Riffat (1996). These studies provide information on the deposition rates of particles in ventilation ducts. Only a few studies have been made on the effect of flow acceleration on microparticle detachment. These involve multi-layer deposits (Fromentin, 1989; Matsusaka & Masuda, 1996) and not individual microparticles.

Microparticle detachment occurs when the moment of the aerodynamic removing forces overcomes that of the adhesion and gravitational forces (Ibrahim, Dunn, & Brach, 2003a; Soltani & Ahmadi, 1994; Ziskind, Fichman, & Gutfinger, 1997). When significant flow acceleration occurs over the microparticle, two additional aerodynamic drag forces, the virtual mass force and the Basset force, can arise. The virtual mass force results from a portion of the fluid immediately adjacent to the microparticle being accelerated with the microparticle. The Basset force (also known as the Boussinesq–Basset force or the history force), accounts for the viscous effects of local fluid acceleration on the microparticle. If these forces are significant, they will increase the aerodynamic drag force on the microparticle. This leads to a decrease in the flow velocity required for detachment. However, for the range of flow accelerations considered in the present study, both forces have negligible effects on the drag force because the density of the microspheres used is approximately 6800 times that of the air (Maxey, 1987).

One mechanism that contributes to microparticle detachment from surfaces in turbulent boundary layers is the burst-sweep event (Blackwelder, 1978; Luchik & Tiederman, 1987; Narahari, Narasimha, & Badri Narayanan, 1971). Burst-sweep events enhance the detachment and entrainment processes by providing larger aerodynamic removing moments (for example, see Rashidi, Hetsroni, & Banerjee, 1990).

The mean flow can be accelerated either *spatially* or *temporally*. Spatial acceleration occurs when an initially turbulent boundary layer is exposed to a large enough favorable pressure gradient over a long enough length. Temporal acceleration occurs when there is a significant increase in flow velocity in time.

Under spatial acceleration, reverse transition (also known as relaminarization) occurs, causing the turbulent boundary layer to revert to a laminar-like state. This relaminarization typically is characterized by a departure of the mean velocity profiles from the "law of the wall" profile, a decrease in the relative turbulence intensity, a decay of the turbulent stresses in the near-wall region and a decline of turbulent burst/sweep events in the wall layer. Considerable research has been done on this type of turbulence suppression (Bourassa, 2005; Narasimha & Sreenivasan, 1973; Patel & Head, 1968; Warnack & Fernholz, 1998).

Similarly, under temporal acceleration, an initially turbulent boundary layer can be relaminarized (Greenblatt & Moss, 1999, 2004). However, compared to the spatial acceleration case, very little is known about the dynamics of this type of flow and how it affects particle detachment. The present work focuses on how *temporally* accelerated flows affect microparticle detachment.

The present study investigates whether rapid temporal acceleration also can delay the transition to turbulence on an initially *laminar* boundary layer and, thereby, affect microparticle detachment. When the flow over a surface is accelerated in time, the boundary layer evolves continuously. If rapid temporal flow accelerations delay the onset of turbulence (like large spatial accelerations reverse turbulent flows to laminar flows), then the wall shear stress, the relative turbulence intensity in the near-wall region, and the frequency and extent of burst-sweep events will be reduced. These, in turn, reduce the instantaneous aerodynamic removing moments local to the microparticle at a given free-stream velocity, thus requiring a larger free-stream velocity to detach the microparticle.

The present study relates directly to three previous publications of the authors (Ibrahim et al., 2003a; Ibrahim, Dunn, & Brach, 2003b; Ibrahim, Dunn, & Brach, 2004). In those studies, the effects of a number of variables on microparticle incipient motion (detachment) were presented and the motion of the microparticles along the surface following detachment was studied. Variables investigated included microparticle shape, density and size, particle residence time on the surface, particle deposition density, particle-surface adhesion energy, fluid relative humidity, fluid final free-stream velocity, fluid final Reynolds number, and slower fluid temporal accelerations. In Ibrahim et al. (2003b), it was reported that relatively slow temporal accelerations (from 0.01 to 0.34 m/s^2) had little effect on microparticle detachment.

The specific aims of the present study are: (1) to determine through measurement whether or not rapid temporal acceleration has an effect on the detachment of microparticles from surfaces, (2) to observe how the flow velocity in the near-wall region, close to where the microparticles are deposited, responds to this rapid temporal acceleration, and (3) to investigate whether or not the production of turbulence is delayed by imposing this kind of flow acceleration, thereby leading to an increase in the free-stream velocity required to detach the microparticles.

In the subject experiments, microspheres were subjected to a controlled acceleration of air flowing over the substrate surface. Stainless steel microspheres, 64–76 μm diameter, were deposited as a sparse monolayer on a smooth surface, initially in a state of static contact equilibrium with a smooth glass substrate. Detachment experiments are conducted at temporal accelerations ranging from 0.01 to 2.0 m/s^2. Larger flow accelerations (from 0.01 to 23 m/s^2) were investigated without the presence of microspheres to document the delay of turbulence production.

2. Description of experiments

Details of the experimental facility and diagnostics used for this study have been described previously (Ibrahim et al., 2003a). Only the features related directly to this study are presented here.

A schematic of the experimental facility is shown in Fig. 1. The facility is an in-draft wind tunnel, with an exhaust fan at its exit. Air is drawn into and through a contraction section, an inlet section, a test section and then, finally, a diffuser section, where it is exhausted into the room. The test section includes a smooth Plexiglas flat plate on its bottom that is 1.05 m long with a leading wedge angle of 10°. The substrate with deposited microparticles is placed in an machined inset designed to interface smoothly with plate. The temperature and relative humidity of the air are measured in the diffuser.

The wind tunnel is equipped with a programmable controller that drives the exhaust fan, which sets both the quasi-steady free-stream velocity, U_∞, and the acceleration during the duration, T, of the transient phase. Decreasing the duration corresponds to an increase in the flow acceleration. For example, at a free-stream velocity of 14.1 m/s, the minimum transient-phase duration allowed by the tunnel's programmable controller is 0.570 s, corresponding to a maximum acceleration of 23 m/s^2. At the maximum duration of 950 s, the corresponding acceleration is 0.01 m/s^2. Fig. 2 displays the progress of the free-stream velocity versus time for five accelerations ranging from 0.01 to 23 m/s^2. The *mean* temporal flow acceleration, α, is defined as a linear approximation to the actual velocity-time record, where $\alpha = (U_{\infty,B} - U_{\infty,A})/(T_B - T_A)$.
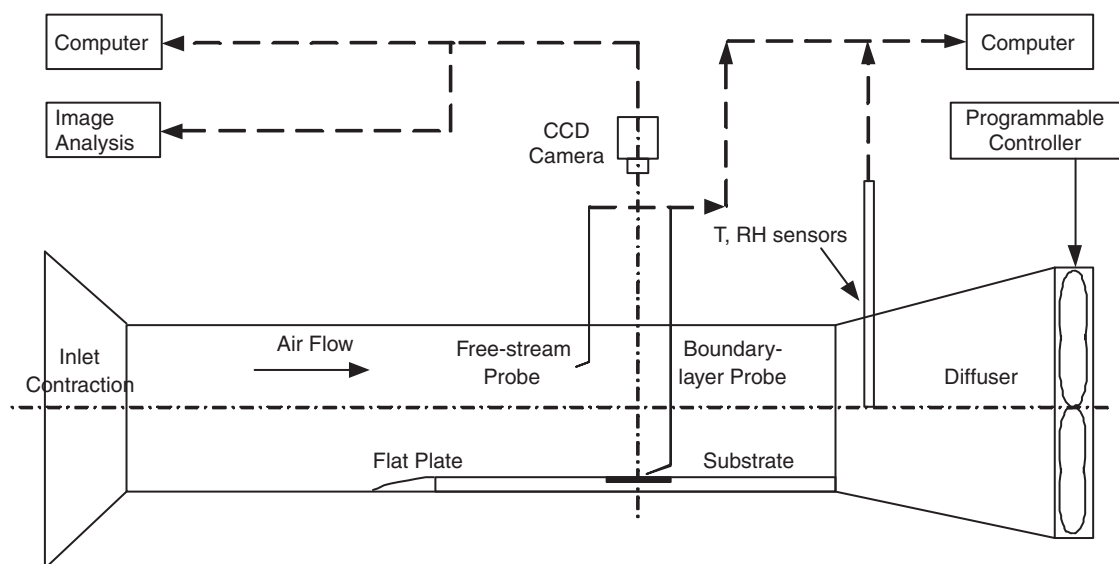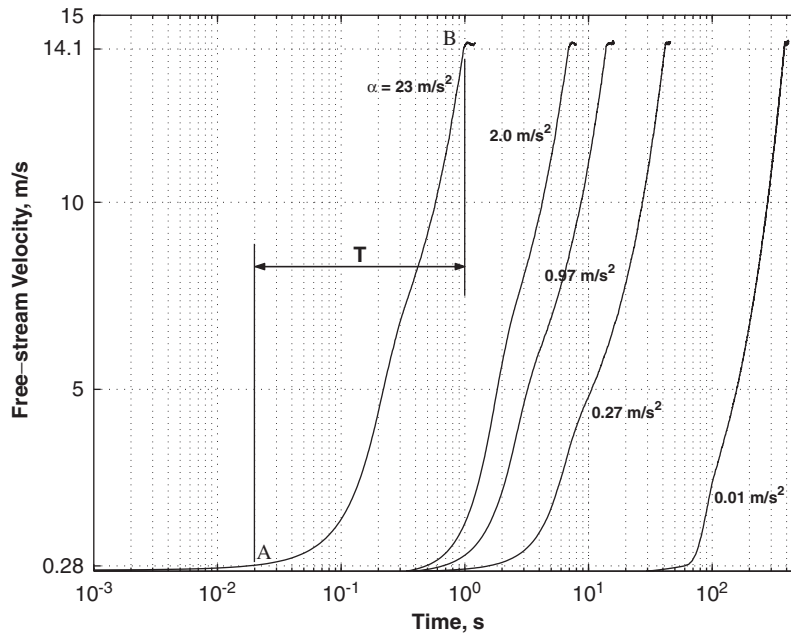

Fig. 1. A schematic of the experimental facility.

Fig. 2. Free-stream velocity versus time for $\alpha = 23$, 2.0, 0.97, 0.27 and 0.01 m/s^2. The final free-stream velocity is 14.1 m/s for all cases.

Two series of experiments were conducted, one to characterize the flow itself, and the other the extent of microparticle detachment resulting from the flow. The first series on flow characterization was done over a range of temporal accelerations from 0.01 to 23 m/s^2 without microparticles present on the substrate. Its results are summarized in Figs. 2–4. The second series was conducted with microparticles present on the substrate over a narrower range of temporal accelerations from 0.01 to 2.0 m/s^2. This results of this series are shown in Figs. 5 and 6.

2.1. Flow characterization

Temporal accelerations for the flow characterization series ranged from 0.01 to 23 m/s^2. Several characteristic flow parameters were quantified using hot-wire anemometry. The free-stream turbulence intensity was measured to be less than 1% over the tunnel's entire operational velocity range. Transient velocity profiles were acquired and found to be repeatable to within 3%. Turbulent boundary layer velocity profiles obtained at different constant velocities were found to agree reasonably to the classic turbulent boundary layer velocity profile data of Klebanoff (1955).

The friction velocity, u^*, characterizes the flow conditions local to the microparticle. It is defined as $\sqrt{\tau_w/\rho}$, where τ_w is the wall shear stress and ρ is the density of the flowing medium. It was correlated with the free-stream velocity, U_∞, using a *static* calibration method (Ibrahim et al., 2003a). The resulting relation was u^* (m/s) $= 0.0375U_\infty + 0.0387$, with an uncertainty in u^* of 0.0300 m/s at 95% confidence.

Two single hot-wire probes (1 mm long and 5 μm diameter; Auspex Model AHWU-100) were placed in the flow, one in the free-stream at the tunnel centerline, and the other in the boundary layer as close to the wall as possible. This distance was approximately 80 μm above the wall (corresponding to a value of the inner variable $y^+ \equiv yu^*/v = 2.8$ at $U_\infty = 14.1$ m/s with fully developed turbulent flow). The probes were calibrated using a pitot-static tube that was connected in parallel to a differential pressure transducer (Setra Model 264) and a manometer containing a fluid-level indicator (Dwyer Model 1430). The probes were held rigidly in place so that no significant motion took place between the probe and the wall during rapid temporal flow accelerations.

The free-stream and boundary layer velocities were acquired using a two-channel hot-wire anemometer (TSI Inc. Model IFA-100). The hot-wire frequency response was set to approximately 10 kHz. The anemometer signal was low-pass filtered at 5 kHz, amplified, then digitized (National Instrument Model NI 6229M). The sampling rates and times were set such that a significant over sampling is obtained at any acceleration. These ranged from 1 kHz and 1200 s at $\alpha = 0.01$ m/s^2 to 100 kHz and 2.5 s at $\alpha = 23$ m/s^2.
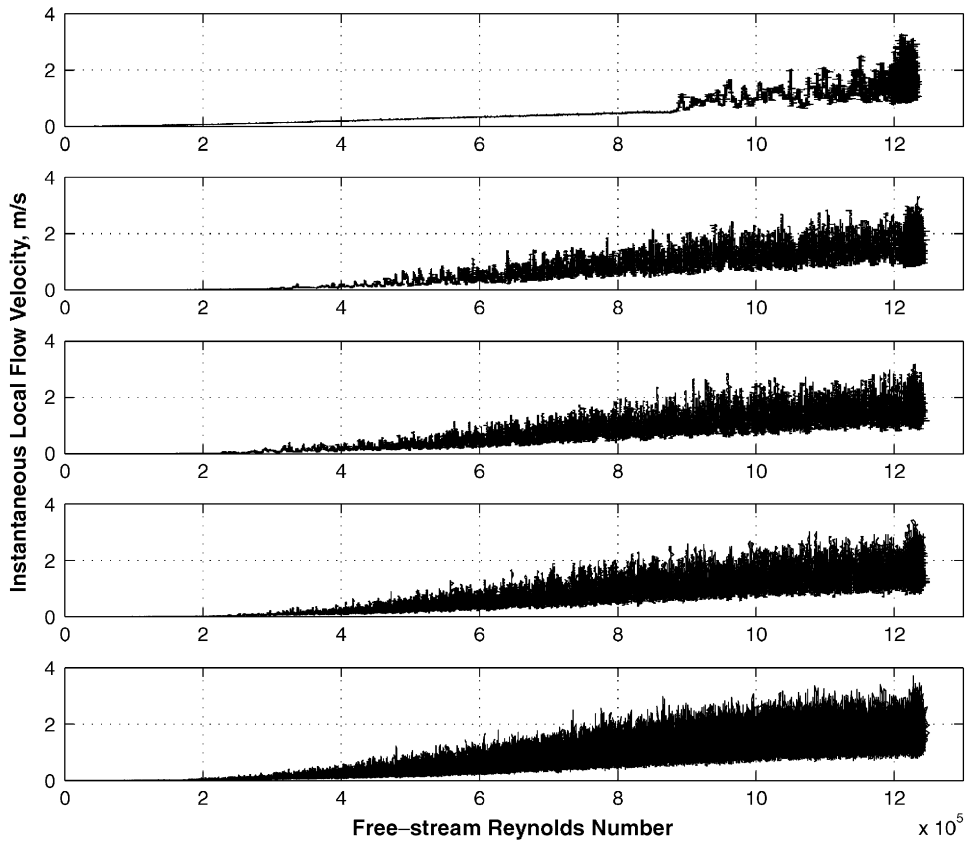
Fig. 3. A comparison between the measured *instantaneous* boundary layer velocity at five temporal mean flow accelerations at a final free-stream velocity of 14.1 m/s and a height of 80 μm above the wall. Acceleration cases from top to bottom are 23, 2.0, 0.97, 0.27 and 0.01 m/s^2, respectively.
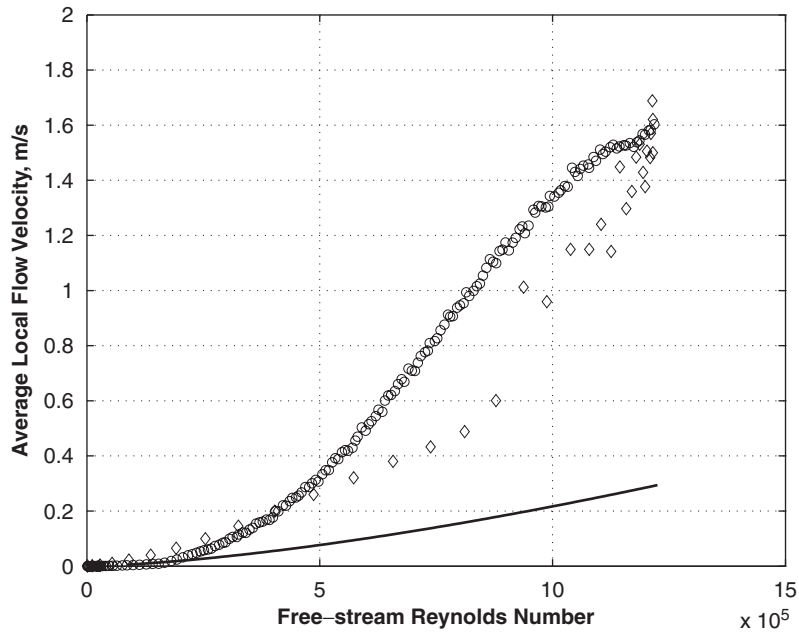

Fig. 4. Measured *mean* local flow velocities at a height of 80 μm above the wall for the temporal mean flow accelerations of 0.01 m/s^2 (open circles) and 23.0 m/s^2 (open diamonds). Every point represents the average of 4000 points. The solid curve denotes the velocity values predicted from laminar boundary layer theory.
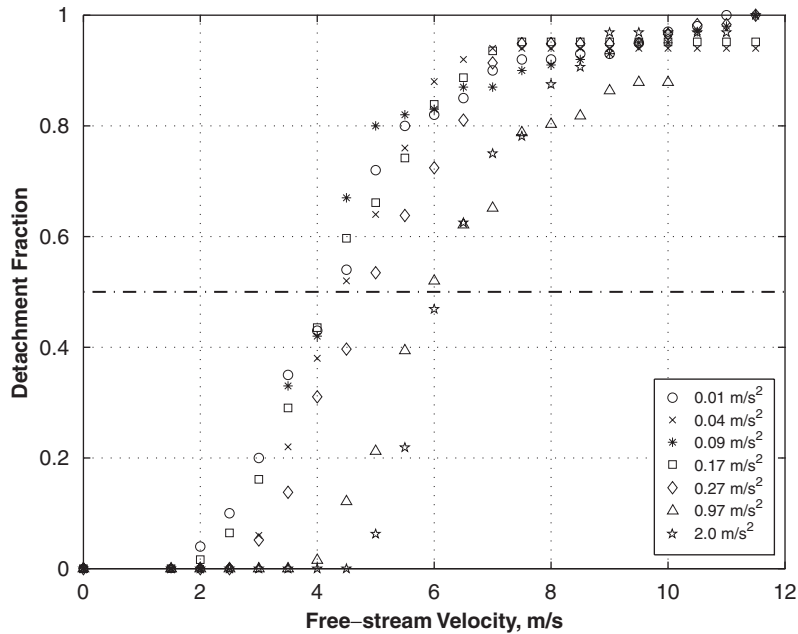
Fig. 5. The progress of the microparticle detachment fraction versus free-stream velocity for seven different accelerations ranging from $\alpha = 0.01$ to $2.0 \, \text{m/s}^2$.

2.2. Microparticle detachment

For this series of experiments, the temporal accelerations varied from 0.01 to 2.0 m/s^2. All experiments were conducted at a temperature of 23 °C $\pm$ 1 °C and a relative humidity of 30% $\pm$ 3%. The experiments of Rashidi et al. (1990) support that microparticles with sizes and loadings comparable to those used in the present study do not modify the turbulence in the near-wall region. Thus, for the present experiments, the turbulence affects the microparticles and not *vice versa*.

The extent of microparticle detachment was characterized through the detachment fraction versus the free-stream velocity. This fraction is defined as $n^*(t) = 1 - [n(t)/n(0)]$, where $n(t)$ is the number of non-detached microspheres on the surface at time t. The free-stream velocity at which $n^*(t)$ equals 0.5 is defined as the free-stream velocity for detachment, $U_{\text{th},\infty}$. The uncertainty in $U_{\text{th},\infty}$, under controlled conditions was approximately 15% (Ibrahim et al., 2003b).

Stainless steel microspheres (Duke Scientific; diameter: 64–76 μm; density: 8000 kg/m^3; Poisson's ratio: 0.28; Young's modulus: 215 GPa), were used. The microspheres were deposited by gravitational settling from a height of approximately 10 cm at a location 1.4 m downstream from the wind tunnel inlet. They were distributed as a sparse monolayer ($\sim$ 50 microspheres/cm^2) unto a glass substrate (Amersham Pharmacia; 10 cm $\times$ 10.5 cm $\times$ 1.27 mm) several minutes before conducting each experiment. Sparse deposition assured minimal collisions with other microspheres following detachment and negligible particle disturbance of the flow field (Ibrahim et al., 2003a).

Similar glass substrates were used for all cases. The substrate was prepared prior to each experiment by cleaning it with phosphate-free detergent, immersing it in dilute nitric acid (1:1) for 60 s, rinsing it in distilled water for 120 s and then heating it at 200 °C for 1 h. All prepared substrates were kept in a dry, warm enclosure until used. The surface-preparation technique was similar to that given by Phares, Smedley, and Flagan (2000).

A glass substrate surface was scanned using an atomic force microscope. The average standard deviation of the surface roughness height was 17 Å, based upon of 10 000 samples. Using the theory of Cheng, Brach, and Dunn (2002), this yielded a 99% reduction in the microsphere/surface adhesion force, which is typical for such surfaces.

The motion of the microparticles was recorded using an analog 0.5 in CCD camera (Astrovid Model 2000, 30 frames/s, 640 pixel $\times$ 480 pixel resolution, 8.4 μm $\times$ 9.8 μm pixel size). An 80 mm optical lens (Olympus) was attached to
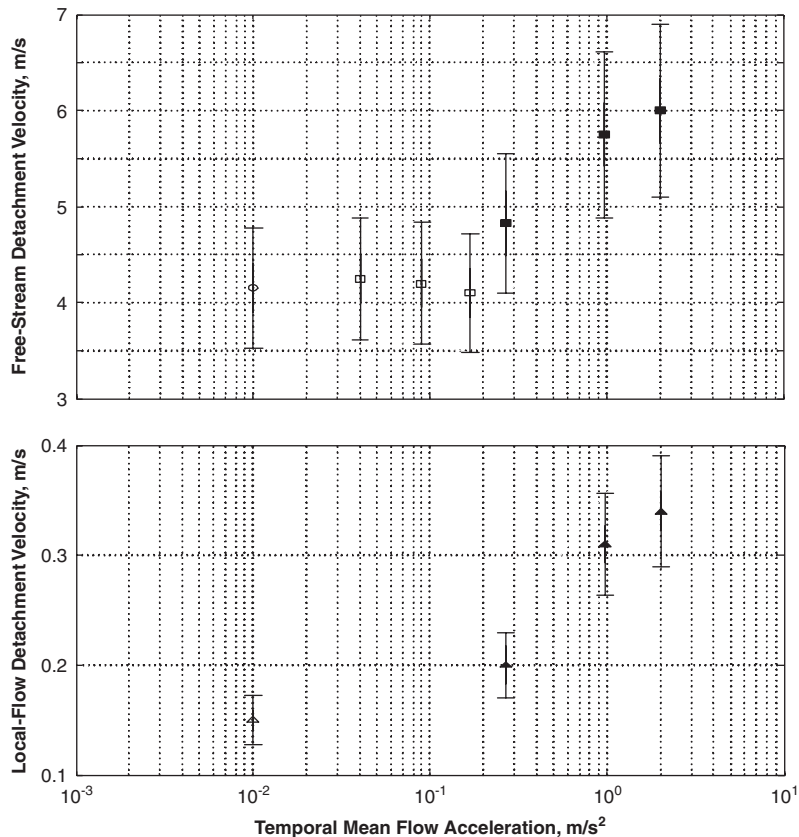
Fig. 6. Variation of the free-stream (top graph with circle and squares) and local-flow (bottom graph with triangles) threshold velocities for detachment with the temporal mean flow acceleration. Open symbols denote microparticle detachment experiment results and closed symbols flow characterization experiment results. Open square symbols are results from Ibrahim et al. (2003b). Local flow velocities were measured 80 μm from the wall.

the camera to achieve enough optical magnification to resolve individual microparticle motion. The camera output was connected to a digitizer and a frame grabber in a personal computer for image analysis. The field of view was 13.7 mm × 10.2 mm under an optical magnification ratio of 21:1. The microparticles were illuminated by a 75 W light bulb. A second computer, synchronized to the first computer using a flash generated by a square-wave input, recorded the free-stream hot-wire anemometer's output versus time. Due to synchronization limits, the maximum temporal flow acceleration that was investigated with microparticles present on the substrate was $2.0 \, \text{m/s}^2$.

3. Results and discussion

Direct evidence of the effect of temporal flow acceleration on the velocities influencing detachment can be seen by examining the instantaneous local flow velocities in the boundary layer near the surface. These are shown in Fig. 3, in which the *instantaneous* local flow velocity at a distance of approximately 80 μm from the surface is plotted for five different accelerations versus the free-stream Reynolds number, Re_{FS}. This Reynolds number is proportional to the free-stream velocity and equals $U_\infty x / v$, where x is the distance from the leading edge of the plate (1.4 m) and v is the kinematic viscosity of the air ($1.6 \times 10^{-5} \, \text{m}^2/\text{s}$). The highest-acceleration case ($\alpha = 23 \, \text{m/s}^2$) specifically was investigated to show the marked differences that are caused by high temporal acceleration. This can been seen by comparing this case with the case of $\alpha = 2.0 \, \text{m/s}^2$. At $Re_{FS} = 800\,000$, for example, the flow is turbulent for $\alpha = 2.0 \, \text{m/s}^2$ but still laminar for $\alpha = 23 \, \text{m/s}^2$ *at the same free-stream velocity*. The transition from laminar to turbulent flow occurs at approximately $Re_{FS} = 200\,000$ for the most slowly-accelerated case ($\alpha = 0.01 \, \text{m/s}^2$). This transition is delayed

to $Re_{FS} = 900\,000$ for the most rapidly-accelerated case ($\alpha = 23\,\text{m/s}^2$). For the four lowest-acceleration cases, from $\alpha = 0.01$ to $2.0\,\text{m/s}^2$, there are smaller but measurable differences in the local flow velocity for the same free-stream Reynolds number. This result suggests that rapid temporal flow acceleration can delay the onset of turbulence. This is similar to reversing a turbulent flow to laminar state using a large spatial acceleration. This observation, therefore, is consistent with the results of Greenblatt and Moss (1999, 2004). The data presented in Fig. 3 is direct evidence that the transition to turbulence is postponed in the near-wall region, at distances as small as approximately twice the radius of the particles used in this study.

The *average* (mean) local flow velocity versus the free-stream Reynolds number is presented in Fig. 4 for the minimum and maximum temporal mean flow accelerations examined (0.01 and $23.0\,\text{m/s}^2$). At $Re_{FS} = 800\,000$, the average local flow velocity for the maximum acceleration case is approximately one-half that for the minimum acceleration case ($\sim 0.5\,\text{m/s}$ versus $\sim 1.0\,\text{m/s}$). The theoretical value of the average flow velocity in a laminar boundary layer at this Re_{FS} is approximately $0.15\,\text{m/s}$ (White, 2006). This reduction in average flow velocity with increasing acceleration probably is the consequence of the turbulent boundary layer reverting to a more laminar-like boundary layer. For the $23.0\,\text{m/s}^2$ acceleration case, there is a relatively abrupt increase in the average local flow velocity at $Re_{FS} \sim 850\,000$. This is a manifestation of the laminar-like boundary layer becoming turbulent-like as Re_{FS} is increased. This transition also can be seen in the instantaneous local flow velocity change, as shown in Fig. 3. Further, the differences between the average local flow velocities for different accelerations is greater over a certain range of free-stream Reynolds numbers. This implies that the increase of $U_{\text{th},\infty}$ with α probably will become more significant when detachment occurs within a certain range of $U_{\text{th},\infty}$ (for example, over a range of air relative humidities, microparticle diameters or surface roughnesses).

The progress of microparticle detachment versus free-stream velocity was studied for seven different accelerations, ranging from $\alpha = 0.01$ to $2.0\,\text{m/s}^2$. The results are presented in Fig. 5. A progressive increase in $U_{\text{th},\infty}$ (the free-stream velocity required to attain $n^*(t) = 0.5$) occurs with increasing α beyond approximately $\alpha = 0.20\,\text{m/s}^2$.

The values of the threshold velocities of detachment for these seven cases are displayed with their experimental uncertainties evaluated at 95% confidence in the top graph of Fig. 6. For temporal flow accelerations below approximately $\alpha = 0.3\,\text{m/s}^2$, the threshold velocity is independent of the acceleration to within the experimental uncertainty. This threshold detachment velocity is approximately $4.1\,\text{m/s}$. For accelerations from approximately $\alpha = 0.3\,\text{m/s}^2$ to (at least) $\alpha = 2.0\,\text{m/s}^2$, $U_{\text{th},\infty}$ is dependent upon and increases with increasing temporal flow acceleration. The threshold detachment velocities are 4.8, 5.8, and $6\,\text{m/s}$ for values of α corresponding to temporal accelerations of 0.27, 0.97 and $2.0\,\text{m/s}^2$, respectively. In this range, $U_{\text{th},\infty}$ increases with α even when considering the measurement uncertainty.

Local flow velocity measurements were made in the near-wall region to investigate the cause of the observed increase in $U_{\text{th},\infty}$ with α. The measured local flow velocities at a height of approximately $80\,\mu\text{m}$ above the wall corresponding the aforementioned free-stream threshold detachment velocities also are presented in the bottom graph of Fig. 6. These were 0.15, 0.20, 0.31 and $0.34\,\text{m/s}$, for temporal accelerations of 0.01, 0.27, 0.97 and $2.0\,\text{m/s}^2$, respectively. Thus, the detachment velocities, based upon either free-stream or local velocities, increase with increasing temporal acceleration. The effect of this increase is evident for accelerations greater than approximately $0.3\,\text{m/s}^2$. One plausible explanation for this increase is that rapid temporal acceleration delays the onset of turbulence, and, therefore, reduces the wall shear stress as well as diminishes the frequency and extent of turbulent burst-sweep events near the wall. This subsequently requires a greater local velocity to achieve the same detachment fraction.

4. Summary and conclusions

The detachment of $70\,\mu\text{m}$-diameter particles from surfaces by air flow was studied under different *temporal* accelerations ranging from 0.01 to $2.0\,\text{m/s}^2$. Additional flow-characterization experiments were conducted up to accelerations of $23\,\text{m/s}^2$. Near-wall hot-wire measurements provided evidence that temporal flow acceleration, like spatial flow acceleration, postponed the transition to turbulence. This reduced the wall shear stress and burst-sweep events in the near-wall region, thereby suppressing detachment. Microparticle detachment experiments revealed that this effect, considering the experimental uncertainties, was observed for accelerations greater than approximately $0.3\,\text{m/s}^2$ (at least up to $2.0\,\text{m/s}^2$).

Acknowledgment

References

Adam, N., Everitt, P., & Riffat, S. B. (1996). Aerosol deposition in ventilation ducts. *International Journal of Energy Research*, *20*, 1095–1101.

Blackwelder, R. F. (1978). The bursting process in turbulent boundary layers. In C. R. Smith, & D. E. Abbott (Eds.), *Coherent structure of turbulent boundary layers*, AFOSR/Lehigh University, Bethlehem, PA.

Bourassa, C. (2005). *An experimental investigation of an accelerated turbulent boundary layer*. Ph.D. Dissertation, University of Notre Dame.

Cheng, W., Brach, R. M., & Dunn, P. F. (2002). Surface roughness effects on microparticle adhesion. *Journal of Adhesion*, *78*, 929–965.

Fromentin, A. (1989). *Particle resuspension from a multi-layer deposit by turbulent flow*. Ph.D. Dissertation, Paul Scherrer Institute, Report Number 38.

Gillette, D. (1978). A wind tunnel simulation of the erosion of soil: Effect of soil texture, sandblasting, wind speed, and soil consolidation on dust production. *Atmospheric Environment*, *12*, 1735–1743.

Greenblatt, D., & Moss, E. A. (1999). Pipe-flow relaminarization by temporal acceleration. *Physics of Fluids*, *11*, 3478–3481.

Greenblatt, D., & Moss, E. A. (2004). Rapid temporal acceleration of a turbulent pipe flow. *Journal of Fluid Mechanics*, *514*, 65–75.

Ibrahim, A. H., Dunn, P. F., & Brach, R. M. (2003a). Microparticle detachment from surfaces exposed to turbulent air flow: Controlled experiments and modeling. *Journal of Aerosol Science*, *34*, 765–782.

Ibrahim, A. H., Dunn, P. F., & Brach, R. M. (2003b). Microparticle detachment from surfaces exposed to air flow: Effects of several factors. *Journal of Aerosol Science*, *35*, 805–821.

Ibrahim, A. H., Dunn, P. F., & Brach, R. M. (2004). Microparticle detachment from surfaces exposed to turbulent air flow: Microparticle motion after detachment. *Journal of Aerosol Science*, *35*, 1189–1204.

Klebanoff, P. S. (1955). *Characteristics of turbulence in a boundary layer with zero pressure gradient*. NACA Technical Report 1247 ⟨http://naca.larc.nasa.gov/⟩.

Luchik, T. S., & Tiederman, W. G. (1987). Timescale and structure of ejections and bursts in turbulent channel flows. *Journal of Fluid Mechanics*, *174*, 529–552.

Matsusaka, S., & Masuda, H. (1996). Particle reentrainment from a fine powder layer in a turbulent air flow. *Journal of Aerosol Science*, *24*, 69–84.

Maxey, M. R. (1987). The motion of a small rigid sphere in a nonuniform flow. *Physics of Fluids*, *30*, 1579–1582.

Narahari, R. K., Narasimha, R., & Badri Narayanan, M. A. (1971). The bursting phenomenon in a turbulent boundary layer. *Journal of Fluid Mechanics*, *48*, 339–352.

Narasimha, R., & Sreenivasan, K. R. (1973). Relaminarization in highly accelerated turbulent boundary layers. *Journal of Fluid Mechanics*, *61*, 417–447.

Nicholson, K. W. (1988). A review of particle resuspension. *Atmospheric Environment*, *22*, 2639–2651.

Patel, V. C., & Head, M. R. (1968). Reversion of turbulent to laminar flows. *Journal of Fluid Mechanics*, *34*, 371–392.

Phares, D. J., Smedley, G. T., & Flagan, R. C. (2000). Effect of particle size and material properties on aerodynamic resuspension from surfaces. *Journal of Aerosol Science*, *31*, 1335–1354.

Rashidi, M., Hetsroni, G., & Banerjee, S. (1990). Particle-turbulence interaction in a boundary layer. *International Journal of Multiphase Flow*, *16*, 935–949.

Sehmel, G. A. (1980). Particle resuspension: A review. *Environment International*, *4*, 107–127.

Siegel, J. A., & Nazaroff, W. W. (2003). Predicting particle deposition on HVAC heat exchangers. *Atmospheric Environment*, *37*, 5587–5596.

Sippola, M. R., & Nazaroff, W. W. (2003). Modeling particle loss in ventilation ducts. *Atmospheric Environment*, *37*, 5597–5609.

Sippola, M. R., & Nazaroff, W. W. (2004). Experiments measuring particle deposition from fully developed turbulent flow in ventilation ducts. *Aerosol Science and Technology*, *38*, 914–925.

Sippola, M. R., & Nazaroff, W. W. (2005). Particle deposition in ventilation ducts: Connectors, bends and developing turbulent flow. *Aerosol Science and Technology*, *39*, 139–150.

Smedley, G. T., Phares, D. J., & Flagan, R. C. (1999). Entrainment of fine particles from surfaces by gas jets impinging at normal incidence. *Experiments in Fluids*, *26*, 324–334.

Smedley, G. T., Phares, D. J., & Flagan, R. C. (2001). Entrainment of fine particles from surfaces by gas jets impinging at oblique incidence source. *Experiments in Fluids*, *30*, 135–142.

Soltani, M., & Ahmadi, G. (1994). On particle adhesion and removal mechanisms in turbulent flows. *Journal of Adhesion Science and Technology*, *8*, 763–785.

Warnack, D., & Fernholz, H. F. (1998). The effects of a favorable pressure gradient and of the Reynolds number on an incompressible axisymmetric turbulent boundary layer, Part 2. *Journal of Fluid Mechanics*, *359*, 357–381.

White, F. M. (2006). *Viscous fluid flow*. (3rd ed.), New York: McGraw-Hill.

Ziskind, G., Fichman, M., & Gutfinger, C. (1995). Resuspension of particulates from surfaces to turbulent flows: Review and analysis. *Journal of Aerosol Science*, *26*, 613–644.

Ziskind, G., Fichman, M., & Gutfinger, C. (1997). Adhesion moment model for estimating particle detachment from a surface. *Journal of Aerosol Science*, *28*, 623–634.